Article

Cancer Cell

# Antagonistic Human FcγRIIB (CD32B) Antibodies Have Anti-Tumor Activity and Overcome Resistance to Antibody Therapy In Vivo

## Graphical Abstract

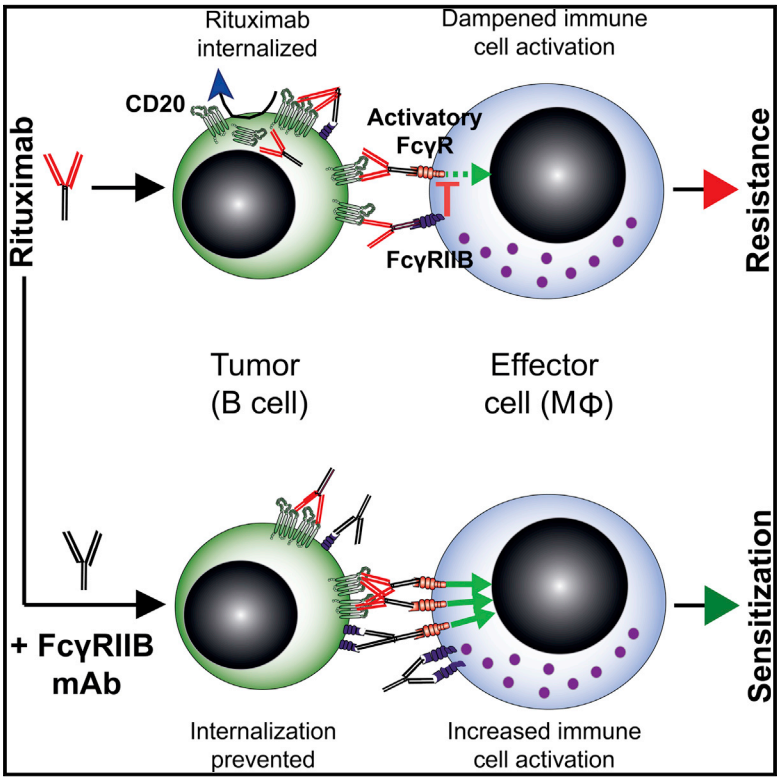


## Authors

Ali Roghanian, Ingrid Teige, ..., Björn Frendéus, Mark S. Cragg

## Correspondence

msc@soton.ac.uk

## In Brief

Roghanian et al. show that antibodies blocking FcγRIIB prevent internalization of anti-CD20 antibody rituximab, thereby maximizing immune effector cell-mediated antitumor activity. Combined targeting of FcγRIIB and CD20 is effective in xenografts from human malignancies clinically relapsed/refractory to rituximab.

## Highlights

- Fully human hFcγRIIB (CD32B) antibodies overcome resistance to therapeutic antibodies
- hFcγRIIB mAbs augment standard-of-care anti-CD20 therapy in vitro and in vivo
- hFcγRIIB mAbs restore drug responsiveness in refractory CLL cells in vivo
- hFcγRIIB mAbs help overcome cell- and niche-specific resistance mechanisms

Roghanian et al., 2015, Cancer Cell *27*, 473–488
April 13, 2015 
http://dx.doi.org/10.1016/j.ccell.2015.03.005

CellPress

Cancer Cell
Article

CellPress

# Antagonistic Human FcγRIIB (CD32B) Antibodies Have Anti-Tumor Activity and Overcome Resistance to Antibody Therapy In Vivo

Ali Roghanian,[1,7] Ingrid Teige,[2,7] Linda Mårtensson,[2] Kerry L. Cox,[1] Mathilda Kovacek,[2] Anne Ljungars,[2] Jenny Mattson,[2] Annika Sundberg,[2] Andrew T. Vaughan,[1] Vallari Shah,[1] Neil R. Smyth,[3] Bhavwanti Sheth,[3] H.T. Claude Chan,[1] Zhan-Chun Li,[2] Emily L. Williams,[1] Giusi Manfredi,[1] Robert J. Oldham,[1] C. Ian Mockridge,[1] Sonya A. James,[1] Lekh N. Dahal,[1] Khiyam Hussain,[1] Björn Nilsson,[4] J. Sjef Verbeek,[5] Gunnar Juliusson,[6] Markus Hansson,[6] Mats Jerkeman,[6] Peter W.M. Johnson,[1] Andrew Davies,[1] Stephen A. Beers,[1] Martin J. Glennie,[1] Björn Frendéus,[1,2,8] and Mark S. Cragg[1,8,*]

[1]Antibody & Vaccine Group, Cancer Sciences Unit, Faculty of Medicine, University of Southampton, Southampton General Hospital, Southampton SO16 6YD, UK
[2]BioInvent International AB, Sölvegatan 41, 22370 Lund, Sweden
[3]Centre for Biological Sciences, University of Southampton, Southampton SO16 6YD, UK
[4]Division of Hematology and Transfusion Medicine, Department of Laboratory Medicine, Lund University, 221 85 Lund, Sweden
[5]Department of Human Genetics, Leiden University Medical Centre, Albinusdreef 2, 2333 ZA Leiden, the Netherlands
[6]Skåne University Hospital, Lund University, 221 84 Lund, Sweden
[7]Co-first author
[8]Co-senior author
*Correspondence: msc@soton.ac.uk
http://dx.doi.org/10.1016/j.ccell.2015.03.005

## SUMMARY

**Therapeutic antibodies have transformed cancer therapy, unlocking mechanisms of action by engaging the immune system. Unfortunately, cures rarely occur and patients display intrinsic or acquired resistance. Here, we demonstrate the therapeutic potential of targeting human (h) FcγRIIB (CD32B), a receptor implicated in immune cell desensitization and tumor cell resistance. FcγRIIB-blocking antibodies prevented internalization of the CD20-specific antibody rituximab, thereby maximizing cell surface accessibility and immune effector cell mediated antitumor activity. In hFcγRIIB-transgenic (Tg) mice, FcγRIIB-blocking antibodies effectively deleted target cells in combination with rituximab, and other therapeutic antibodies, from resistance-prone stromal compartments. Similar efficacy was seen in primary human tumor xenografts, including with cells from patients with relapsed/refractory disease. These data support the further development of hFcγRIIB antibodies for clinical assessment.**

## INTRODUCTION

Biological therapies, and monoclonal antibodies (mAbs) in particular, are an expanding class of therapeutics (Reichert and Dhimolea, 2012). They have revolutionized cancer therapy and become standard of care alongside conventional chemotherapy for several malignancies. Their activity is governed by interaction with Fc gamma receptors (FcγR). Specifically, the relative expression level, affinity, and activity of the FcγR explains much of their efficacy (Nimmerjahn and Ravetch, 2008, 2011). Much less is known of the mechanisms underlying intrinsic or acquired resistance to mAbs. With mAb therapies

### Significance

Therapeutic antibodies have improved cancer treatment, but resistance frequently emerges translating into treatment failure. Antibodies exert antitumor activity by interfering with ligand-receptor signaling pathways and uniquely by orchestrating patient anti-cancer immunity through interaction with immune cell antibody receptors (FcγRs). A single inhibitory antibody receptor expressed on immune cells and certain cancers, FcγRIIB, is implicated in intrinsic and acquired antibody drug resistance and treatment failure in lymphoma and leukemia. We demonstrate that monoclonal antibodies (mAbs) targeting human FcγRIIB overcome this resistance. By blocking FcγRIIB function, these mAbs augmented the activity of several clinically approved therapeutic mAbs and overcame relapsed/refractory disease in vivo. Targeting FcγRIIB could help overcome cancer cell resistance and improve clinical responses with multiple mAb therapies.

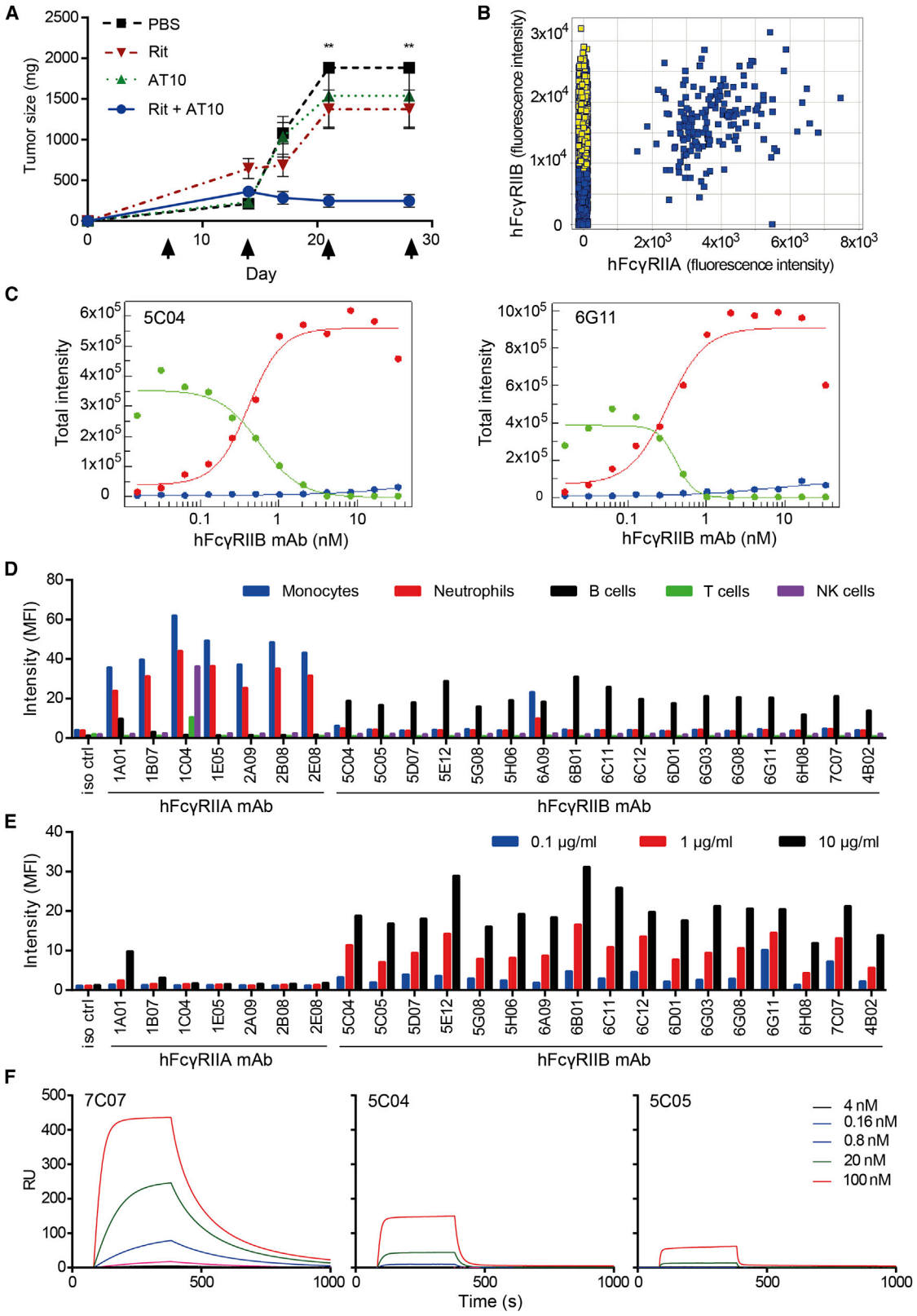


**Figure 1. Therapeutic Effects of hFcγRII mAb (AT10) and Generation of Specific mAbs Capable of Distinguishing hFcγRIIB and hFcγRIIA**

(A) SCID mice (five per group) xenografted with Daudi cells (s.c.) were treated (i.p.) as indicated by arrows. Mean tumor weights plotted ± SEM and analyzed using unpaired t test; p values compare rituximab (Rit) alone versus Rit + AT10-treated groups (**$p \leq 0.005$). Representative data (n = 2).

*(legend continued on next page)*

increasingly being developed, there is an urgent need to understand resistance and to develop drugs to overcome it. Because several anti-cancer mAbs depend on engaging mAb-dependent immune cell-mediated anti-tumor mechanisms for preclinical (Beers et al., 2010; Clynes et al., 2000; Hamaguchi et al., 2006; Minard-Colin et al., 2008) and clinical efficacy (Cartron et al., 2002; Dyer et al., 1989; Weng and Levy, 2003), there is a need to understand and prevent resistance to them.

Rituximab is a type I hCD20 mAb approved for cancer immunotherapy and has been widely administered to patients with B cell cancers including follicular lymphoma (FL), diffuse large cell B cell lymphoma (DLBCL), chronic lymphocytic leukemia (CLL), and mantle cell lymphoma (MCL) (Lim et al., 2010). Whereas rituximab is efficacious in FL and DLBCL, improving overall survival, only modest responses are seen in CLL and MCL. Furthermore, even with rituximab-responsive lymphoma sub-types, some individuals show initial resistance or subsequently develop it, making it a clinically relevant system in which to study mAb resistance mechanisms.

We recently demonstrated that the inhibitory FcγRIIB promotes rituximab internalization from B cells (Lim et al., 2011; Vaughan et al., 2014). As the main IgG receptor on B cells, FcγRIIB becomes phosphorylated and removes rituximab from the B cell surface, effectively abrogating all mAb-dependent immune cell anti-cancer mechanisms (Lim et al., 2011). In contrast, so-called type II anti-CD20 mAbs such as the recently approved obinutuzumab (GA101) are not as sensitive to this process, perhaps due to their inability to redistribute CD20 into lipid rafts (Cragg et al., 2003; Lim et al., 2011). FcγRIIB-mediated rituximab internalization correlated with clinical responsiveness (least to most) as CLL < MCL < FL and DLBCL (Lim et al., 2011). In keeping with a role for FcγRIIB in mAb resistance, a retrospective analysis of patients with MCL treated with rituximab immunochemotherapy demonstrated greater survival among patients with FcγRIIB-negative compared with FcγRIIB-positive tumor biopsies (Lim et al., 2011). Similarly poor responses were observed in patients with FL expressing high levels of FcγRIIB when receiving rituximab monotherapy (Lee et al., 2015).

In this study, we investigate the development of specific mAbs to hFcγRIIB, capable of blocking rituximab internalization, and assess their therapeutic potential.

## RESULTS

### Generation and Characterization of hFcγRIIB-Specific mAb

We recently reported that resistance to rituximab in some patients with lymphoma could be explained by its internalization from the tumor and that the expression of the inhibitory FcγRIIB on the target B cell surface promotes this process (Beers et al., 2010; Lim et al., 2011). Consistent with this hypothesis, in vivo co-administration of hFcγRII mAb AT10 with rituximab resulted in additive/synergistic anti-tumor responses in two different lymphoma xenograft models where hCD20 and hFcγRIIB are co-expressed on the tumors (Figures 1A, S1A, and S1B).

The extracellular domain of hFcγRIIB is ~93% homologous to hFcγRIIA, a key activatory FcγR (Figure S1C). Because these receptors mediate opposing functions, it is critical for a therapeutic mAb to be highly specific for hFcγRIIB. AT10 does not fulfill this criterion because it binds both hFcγRIIA and hFcγRIIB (Greenman et al., 1991). To generate hFcγRIIB-specific antibodies with therapeutic potential in humans, we used a human antibody phage-display library n-CoDeR (Söderlind et al., 2000) panning for binding to hFcγRIIB and against binding to hFcγRIIA (or vice versa) to generate mono-specific reagents (Figures 1B–1F). The resultant mAbs were assessed for the ability to selectively bind (Figure 1B) and block immune complex (IC) binding to hFcγRIIB, but not hFcγRIIA (Figure 1C). Leukocyte subset (neutrophils, monocytes, B cells, T cells, and natural killer [NK] cells) screening demonstrated the high specificity of the mAbs for either hFcγRIIB or hFcγRIIA (Figures 1D, 1E, and S1D–S1F). The relative affinities for hFcγRIIB were determined by ELISA (Table S1), with a subset assessed by surface plasmon resonance (SPR) showing $K_D$ for binding to hFcγRIIB in the range of $\sim 1 \times 10^{-7}$ to $2 \times 10^{-8}$ M (Figure 1F and Table S1). Accordingly, 14 highly specific hFcγRIIB mAbs were identified and validated. Although the fine specificity for each mAb has not been defined, they all block IC binding and do not cross-react with FcγRIIA, strongly indicating they bind around the IgG binding cleft, where a high concentration of residues differing between FcγRIIA and B occur (Figure S1C).

### Antagonistic hFcγRIIB mAbs Block Rituximab Internalization

Rituximab engagement on B cells activates hFcγRIIB by phosphorylating its ITIM (Lim et al., 2011; Vaughan et al., 2014). We speculated, based on the immune inhibitory function of hFcγRIIB, that mAbs capable of preventing both CD20 internalization and blocking hFcγRIIB activation/phosphorylation would be of therapeutic interest. To assess effects in a variable domain-dependent manner, we engineered N297Q variants that cannot bind FcγR through their Fc domain (see below) (Tao and Morrison, 1989). Treatment of Raji cells with hFcγRIIB mAbs resulted in two different responses; high levels of ITIM phosphorylation (e.g., 5C04 and 6G08) and little to no effect (e.g., 6G11 and 7C07) (Figure 2A). Similar observations were seen with primary CLL cells, tonsils, and monocytes (Figures S2A and S2B, and data not shown). The varied ability of these mAbs to activate hFcγRIIB is extremely interesting; the epitopes engaged, membrane dynamics and structure:function relationships involved are the focus of our ongoing studies. Nonetheless,

(B) scFv screening for binding to hFcγRIIB (yellow dots) and/or hFcγRIIA (blue).
(C) hFcγRIIB mAb binding to hFcγRIIB- (red line) or hFcγRIIA-transfected cells (blue line) and mAb-dependent inhibition of IC binding to hFcγRIIB-transfected cells (green line).
(D) Binding profile of mAbs on human leukocyte populations.
(E) Dose-dependent binding of mAbs to B cells.
(F) BIAcore assessment of hFcγRIIB mAb binding to hFcγRIIB fusion protein. $K_D$ values calculated from the 1:1 binding model (see Table S1).
See also Figure S1 and Table S1.

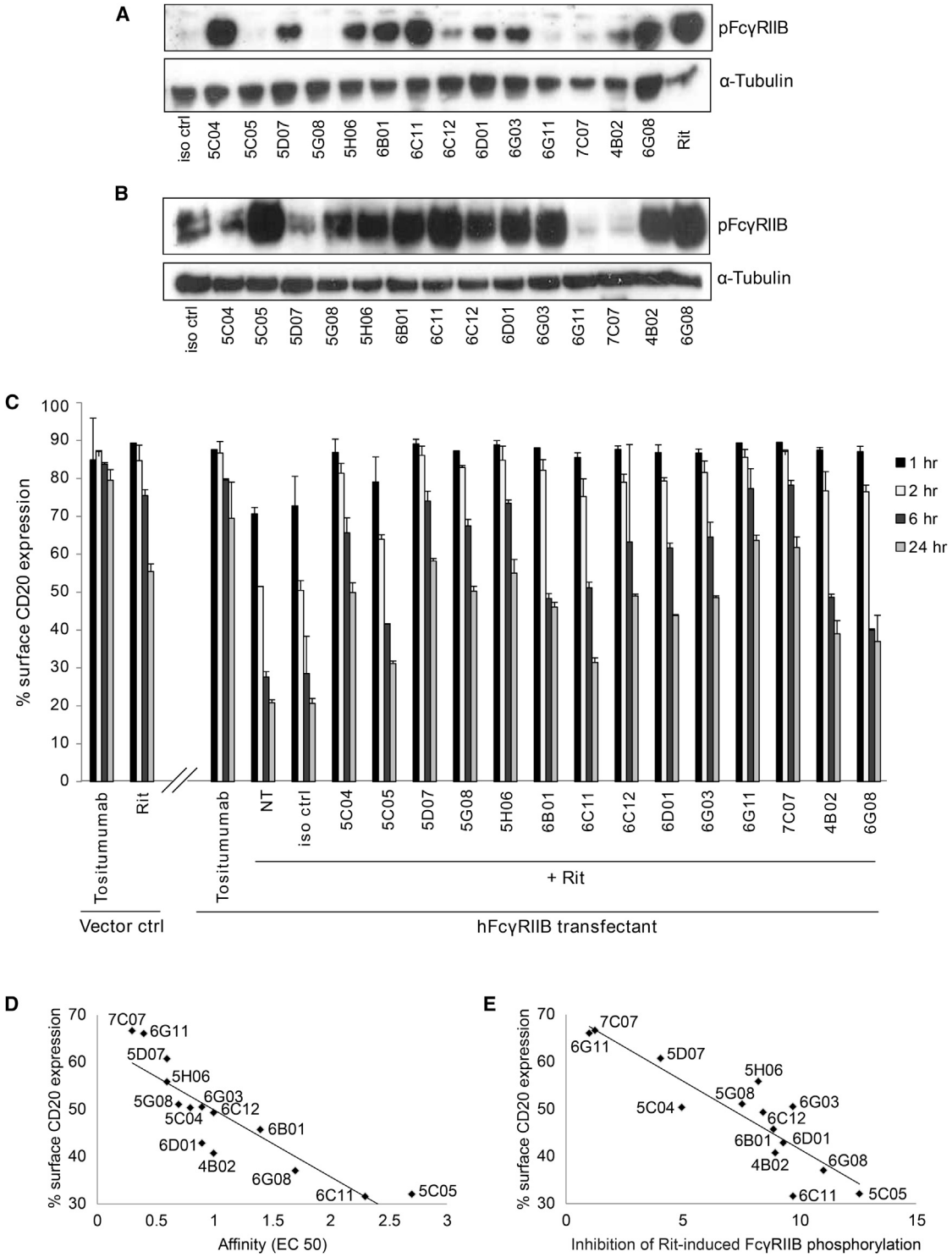


**Figure 2. hFcγRIIB mAbs Are Capable of Blocking Rituximab Engagement with FcγRIIB on the Surface of Target Cells**

(A) Ability of N297Q hFcγRIIB mAbs to elicit hFcγRIIB ITIM phosphorylation (pFcγRIIB) on Raji cells; hIgG1 isotype control (iso ctrl) and Rit used as negative and positive controls, respectively. α-Tubulin loading control.

(B) Ability of N297Q hFcγRIIB mAbs to block hFcγRIIB ITIM phosphorylation induced by Rit. Representative blots (n = 3) shown in (A) and (B).

(C) Ability of N297Q hFcγRIIB mAbs to block internalization induced by Rit. Mean + SD of three independent experiments.

(D) Correlation between the ability of hFcγRIIB mAbs to block Rit internalization (shown in C) and their relative ranked affinities ($R^2$ = 0.78).

(E) Correlation between the ability to block Rit internalization and the ability to block Rit-induced phosphorylation of hFcγRIIB (shown in B) ($R^2$ = 0.79).

See also Figure S2.

the data demonstrate that hFcγRIIB mAbs capable of blocking IC binding without activating the receptor were successfully generated.

Next, we investigated whether hFcγRIIB mAbs could block the interaction between hFcγRIIB and rituximab and prevent rituximab internalization. Some mAbs such as 6G08 remained agonistic, stimulating receptor phosphorylation. In contrast, two mAbs (6G11 and 7C07) referred hereon as antagonistic were able to almost completely prevent the hFcγRIIB phosphorylation induced after rituximab binding (Figure 2B). The same mAbs were able to efficiently block internalization of rituximab from the surface of hFcγRIIB-transfected Ramos cells, similar to the level seen with the type II hCD20 mAb tositumomab and Ramos cells lacking hFcγRIIB (Figure 2C). Both wild-type (WT) and N297Q variants had equivalent activity, indicating a variable domain dependent effect (Figure S2C) and that antagonistic effects were retained with WT hIgG1. The ability to block rituximab internalization correlated with their relative affinity for hFcγRIIB; $R^2$ = 0.78 (Figure 2D), which was in turn correlated to their relative ability to block hFcγRIIB phosphorylation after rituximab stimulation; $R^2$ = 0.79 (Figure 2E). Thus, high-affinity antagonistic hFcγRIIB mAbs prevented hFcγRIIB-mediated removal of rituximab from the target cell surface.

## Antagonistic hFcγRIIB mAb Have Potent Anti-Tumor Activity In Vitro

The finding that the antagonistic effects of some mAbs were retained in the WT hIgG1 format, which productively engages with activatory FcγR-expressing immune cells, suggested that these mAbs might have intrinsic Fc:FcγR-dependent anti-tumor activity. We therefore screened our hFcγRIIB mAbs for such effects. The antagonistic mAbs 7C07 and 6G11 were among the clones that induced the highest antibody-dependent cellular cytotoxicity (ADCC) activity (Figures S3A and S3B). Having established that these two clones had the highest affinity, and strongest activity in blocking rituximab internalization and in eliciting ADCC, we next assessed their binding to a panel of human and animal tissues known to express FcγRs. Both 7C07 and 6G11 specifically stained lymphocytes in human spleen and tonsils, but not lymphocytes in cynomolgus monkeys, rats, rabbits, or mice indicating that these mAbs are not cross-reactive for FcγRIIB in other species (Figure 3A and data not shown). However, clone 7C07, but not 6G11, additionally stained the sinusoids of spleen and LN from various species, indicating an undesired cross-reactivity (Figures 3A and S3C). WT and N297Q 6G11 mAbs were shown to stain equivalently (Figure S3D), and no additional unanticipated cross-reactivity was observed on other human tissues (Figure S3E). Based on this reactivity profile, clone 6G11 was selected as our lead clinical candidate.

The intrinsic cytotoxic activity of 6G11 was further explored in programmed cell death (PCD), antibody-dependent cell phagocytosis (ADCP), and ADCC assays using primary patient CLL samples. Substantial activity was demonstrated in each assay at a level greater than observed with rituximab (Figures 3B–3D). Furthermore, 6G11 was more efficacious compared to rituximab in assays with NK cell effectors expressing either the high- or low-affinity variants of hFcγRIIIA (158V or F, respectively; Ravetch and Perussia, 1989) (Figure 3E).

Subsequently, we examined the ability of 6G11 to prevent the internalization of rituximab from the surface of primary CLL cells. Both WT and N297Q (the latter devoid of intrinsic Fc-dependent effector activity due to an inability to engage FcγR; Figure S3F) variants of 6G11 prevented rituximab internalization (Figure 3F). Unlike hCD20, engagement of hFcγRIIB by either WT or N297Q mAbs (6G11 and AT10) did not result in high levels of hFcγRIIB internalization (Figures 3G, S3G, and S3H).

To address whether 6G11 could also enhance the cytotoxic activity of rituximab by preventing its internalization, we co-incubated primary CLL cells with rituximab and N297Q 6G11 and assessed ADCP and ADCC. N297Q 6G11 was shown to substantially promote the ADCP of rituximab-opsonized CLL cells compared to rituximab alone (Figures 3H and 3I). In these assays, there is no free N297Q 6G11 to bind to the macrophage FcγRIIB, and the N297Q mutation ensures that the Fc region of 6G11 does not interact with the activatory macrophage FcγRs. Similar increases in activity were seen in ADCC assays with NK cells (Figure 3J). NK cells do not express FcγRIIB, confirming that augmentation through hFcγRIIB mAb arises from inhibition of rituximab internalization. These data confirm that blocking hFcγRIIB on the target cell surface inhibits internalization of the mAb:target:hFcγRIIB complex, and augments their deletion by effector cells.

Taken together, these observations suggested that 6G11 can elicit anti-tumor activity through dual mechanisms—intrinsic cytotoxic activity, and potentiation of rituximab activity through prevention of its removal from the cell surface.

## 6G11 Is Well Tolerated, Has Therapeutically Relevant Pharmacokinetics, and Does Not Result in a Cytokine Storm

hFcγRIIB is expressed on both target B cells, where it mediates removal of rituximab from the cell surface, and on key immune effector cells such as macrophages where it dampens anti-cancer mAb responses (Clynes et al., 2000; Hamaguchi et al., 2006; Minard-Colin et al., 2008; Montalvao et al., 2013). To understand the impact of targeting hFcγRIIB systemically on relevant hFcγRIIB-expressing cell-types, we generated mice expressing hFcγRIIB under the control of the native human *FCGR2B* promoter (Figures S4A and S4B). The expression and distribution of hFcγRIIB in the Tg mouse closely resembles that in human tissues being strongly expressed on B lymphocytes, less so on macrophages and monocytes and little to no expression on neutrophils, unlike mouse (m) FcγRII (Figures S4C–S4G and data not shown). Equivalent expression was maintained in the *Fcgr2b*$^{-/-}$ mouse background (hereon mFcγRII$^{-/-}$), allowing us to study the effect of hFcγRIIB in the absence of the endogenous mouse receptor. Importantly, the antagonistic activity of 6G11 was retained in these mice (Figure S4H). In addition, hFcγRIIB expression on endothelial cells was lower than that in WT mice and more similar to that in humans (Figure S4I; Alison L. Tutt, S.A.J., Stéphanie A. Laversin, Thomas R.W. Tipton, M.A.K., Ruth R. French, K.H., A.T.V., Lang Dou, Alexander Earley, Lekh N. Dahal, Chen Lu, Melanie Dunscombe, H.T.C.C., Christine A. Penfold, Jinny H. Kim, Elizabeth Potter, C.I.M., A.R., R.J.O., K.L.C., I.T., B.F., M.J.G., S.A.B., and M.S.C., unpublished data).

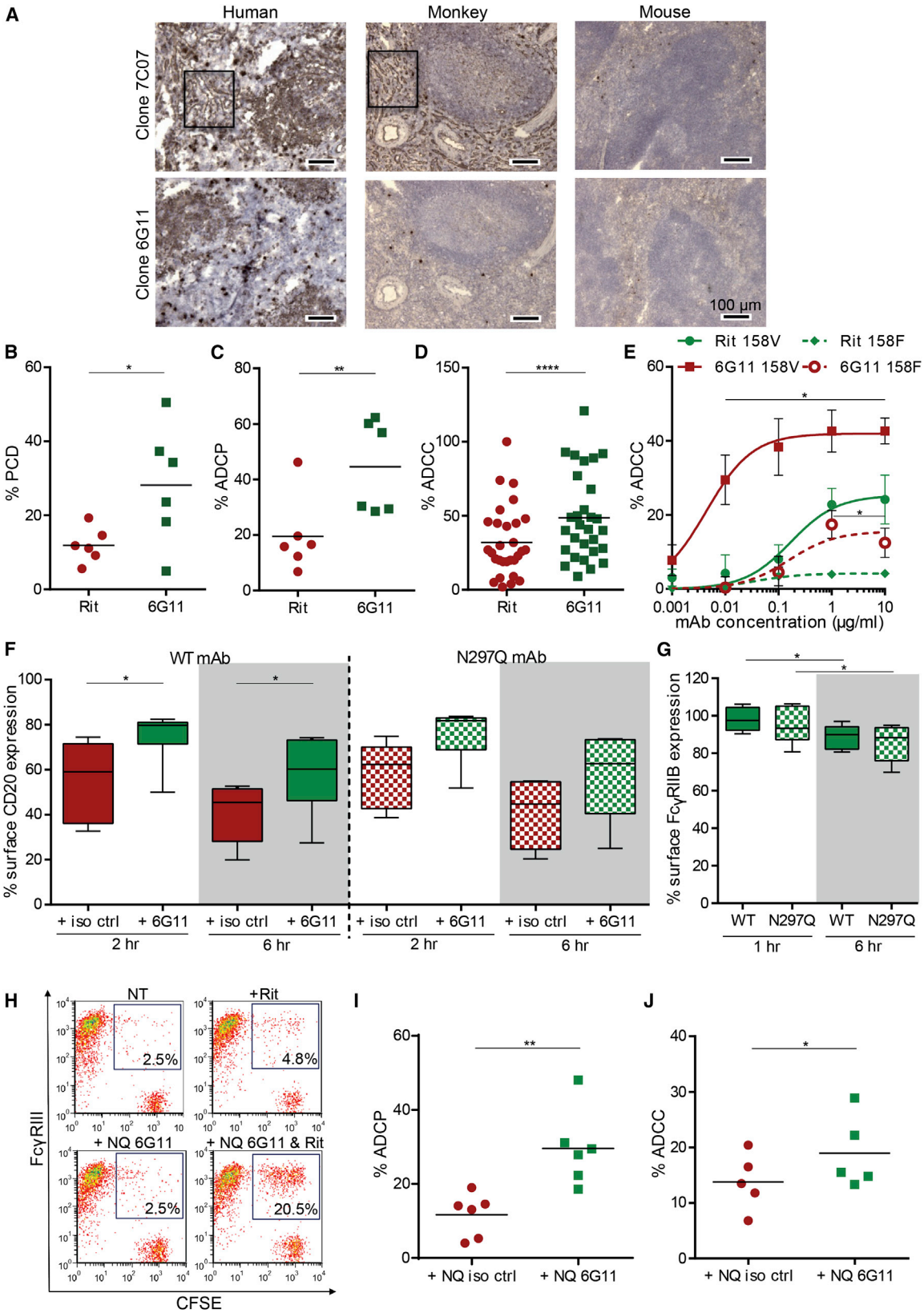


*(legend on next page)*

To ascertain the safety of 6G11 treatment in vivo, we performed a dose-escalation study treating cohorts of hFcγRIIB$^{+/-}$ × mFcγRII$^{-/-}$ mice with 1, 10, or 100 mg/kg 6G11 (Figure S4J). None of the treated mice suffered adverse events such as acute effects, distress, or weight loss (Figure S4K). Tissue examination at day 7 failed to indicate any gross toxicity in the organs (kidney, brain, spleen, liver, lungs). Substantial depletion of hFcγRIIB$^{+}$ B cells was observed both in the blood (Figure 4A) and spleen (Figure 4B) at doses above 1 mg/kg, with equivalent activity in the 10 and 100 mg/kg groups. 6G11 is a fully human mAb easily detected in the sera of mice but inherently immunogenic, so we concurrently assessed its half-life and evidence of mouse anti-human antibody (MAHA) responses. At doses >1 mg/kg, target-mediated clearance that affects the pharmacokinetic (PK) profile was overcome, with little or no effect of target binding in the 10 and 100 mg/kg groups (Figure 4C). However, within 7 days, significant MAHA was observed, resulting in rapid mAb clearance (Figure 4D). Based upon the time-points prior to the advent of significant MAHA, we estimate the mAb half-life to be in the region of 2–4 days for the 10 and 100 mg/kg doses (Figures 4C and 4D and Table S2).

We also performed a repeat dosing study to better mimic how 6G11 might be delivered clinically, administering it four times throughout a 24-day period (Figure S4L) with mice examined as before. Depletion of circulating B cells was observed in hFcγRIIB$^{+/-}$ × mFcγRII$^{-/-}$ but not the mFcγRII$^{-/-}$ control group injected with multiple doses (10 mg/kg) of 6G11 (Figure 4E). Likewise, mice did not suffer weight loss (Figure S4M) or adverse events and no signs of gross toxicity were observed (data not shown). As before, substantial MAHA responses were observed in hFcγRIIB$^{+/-}$ × mFcγRII$^{-/-}$ mice within 1 week and contributed to rapid loss of 6G11 from the serum (Figure 4F). In contrast, no MAHA was detected in the mFcγRII$^{-/-}$ control group, indicating a co-dependence on xenogeneic mAb and surface antigen being required for MAHA induction (Figure 4F).

To explore if hFcγRIIB$^{+}$ cells other than B cells might be deleted after 6G11 treatment, whole blood depletion assays with human blood (Figures 4G–4I) and in vivo experiments with the hFcγRIIB Tg mice (Figure S4N) were performed. B cells but not monocytes or neutrophils were deleted by WT 6G11 IgG1, but not N297Q 6G11. The same lack of depletion of monocytes and neutrophils was seen in combination with rituximab (Figures 4G–4I). Next, we used a recently developed in vitro cytokine release syndrome (CRS) assay (CRA) (Hussain et al., 2015) to assess the potential impact of 6G11 on human peripheral blood mononuclear cells (PBMCs) rendered sensitive to stimulation through high-density culture (Römer et al., 2011) and detected substantial levels of interferon gamma, tumor necrosis factor alpha and/or interleukin 8 following addition of several mAb specificities (CD3, CD28, or CD52) previously highlighted as eliciting CRS. Application of WT or N297Q 6G11 for 48 hr did not result in substantial cytokine release, unlike with 500× lower doses of CD3 mAb (Figure 4J). Similar results were obtained using a whole or diluted blood CRA (Figure S4O).

Collectively, these data demonstrated no adverse effects and indicated a therapeutically relevant PK profile for 6G11 mAb, supporting efficacy studies.

## 6G11 Has Intrinsic Activity and Potentiates Depletion with Rituximab in Immune-Competent Mice

The depleting potential of targeting hFcγRIIB, alone or in combination with rituximab, was then assessed using both 6G11 (hIgG1) and AT10 (mIgG1). First, in short-term adoptive transfer assays, where CFSE$^{+}$ hFcγRIIB$^{+/-}$ × mFcγRII$^{-/-}$ splenocytes were injected into WT recipients and subsequently treated with 6G11 (Figures 5A and 5B) or AT10 (Figure S5A), transferred cells were observed to be efficiently depleted from the circulation and spleen. As little as 0.04 mg/kg mAb was sufficient to elicit ~50% B cell depletion. Depletion was dependent upon Fc:activatory FcγR interaction as activity was lost with F(ab′)$_2$ fragments and N297Q variants; hFcγRIIB$^{+}$ targets were also not deleted in γ chain$^{-/-}$ (γKO) mice, lacking activatory FcγRs (Figures 5A, 5B, and S5A). These data confirm that 6G11 is capable of deleting target cells in vivo, dependent upon the interaction with activatory FcγRs on immune effector cells.

To extend our analysis to combination therapy with rituximab, hCD20$^{+/-}$ × hFcγRIIB$^{+/-}$ × mFcγRII$^{-/-}$ mice were generated. Combination of rituximab and 6G11 (or AT10) resulted in higher depletion of target B cells compared to either mAb alone in assays transferring targets into WT recipients (Figures 5C and S5B, respectively). Similarly, adoptively transferred hCD20$^{+/-}$ × hFcγRIIB$^{+/-}$ × mFcγRII$^{-/-}$ B cells were more effectively depleted by combining rituximab with 6G11 in hFcγRIIB$^{+/-}$ × mFcγRII$^{-/-}$ recipient mice (expressing the hFcγRIIB also on the effector cells) (Figure 5D). As above, treated mice did not suffer weight loss, did not appear to suffer adverse events, and no signs of gross toxicity were observed.

**Figure 3. hFcγRIIB mAb 6G11 Has Potent Cytotoxic Activity In Vitro and Is Capable of Blocking Rit Engagement with hFcγRIIB on the Surface of CLL Cells**

(A) IHC analysis of spleen tissues using 7C07 and 6G11.

(B–D) Cytotoxic ability of 6G11 in PCD (B), ADCP (C), and ADCC (D) using primary CLL cells.

(E) ADCC assay using effector cells expressing the hFcγRIIIA 158F or V allele; mean ± SD (n = 3). Data analyzed with t test comparing samples at the indicated concentrations.

(B–E) In all graphs, the iso ctrl values have been subtracted.

(F) Ability of 6G11 to impair Rit internalization from the surface of CLL cells (n = 6).

(G) Ability of 6G11 to remain at the surface of CLL cells (n = 6).

(F and G) Box-and-whisker plots indicating the upper and lower quartiles with the median shown as the horizontal line and the whiskers showing the maximum and minimum values. Data analyzed using Wilcoxon test.

(H and I) CFSE-labeled CLL cells opsonized for 3–4 hr with Rit ± N297Q iso ctrl or 6G11 before co-culture with MDMs. Representative dot plots shown in (H) and the % of MDMs that have phagocytosed CFSE$^{+}$ CLL cells in (I).

(J) CLL cells opsonized with Rit ± N297Q iso ctrl or 6G11 for 3–4 hr before co-culture with NK cells.

(B–D, I, and J) Mean values shown (horizontal lines) with each dot representing an individual donor. Data analyzed by paired t test. See also Figure S3.

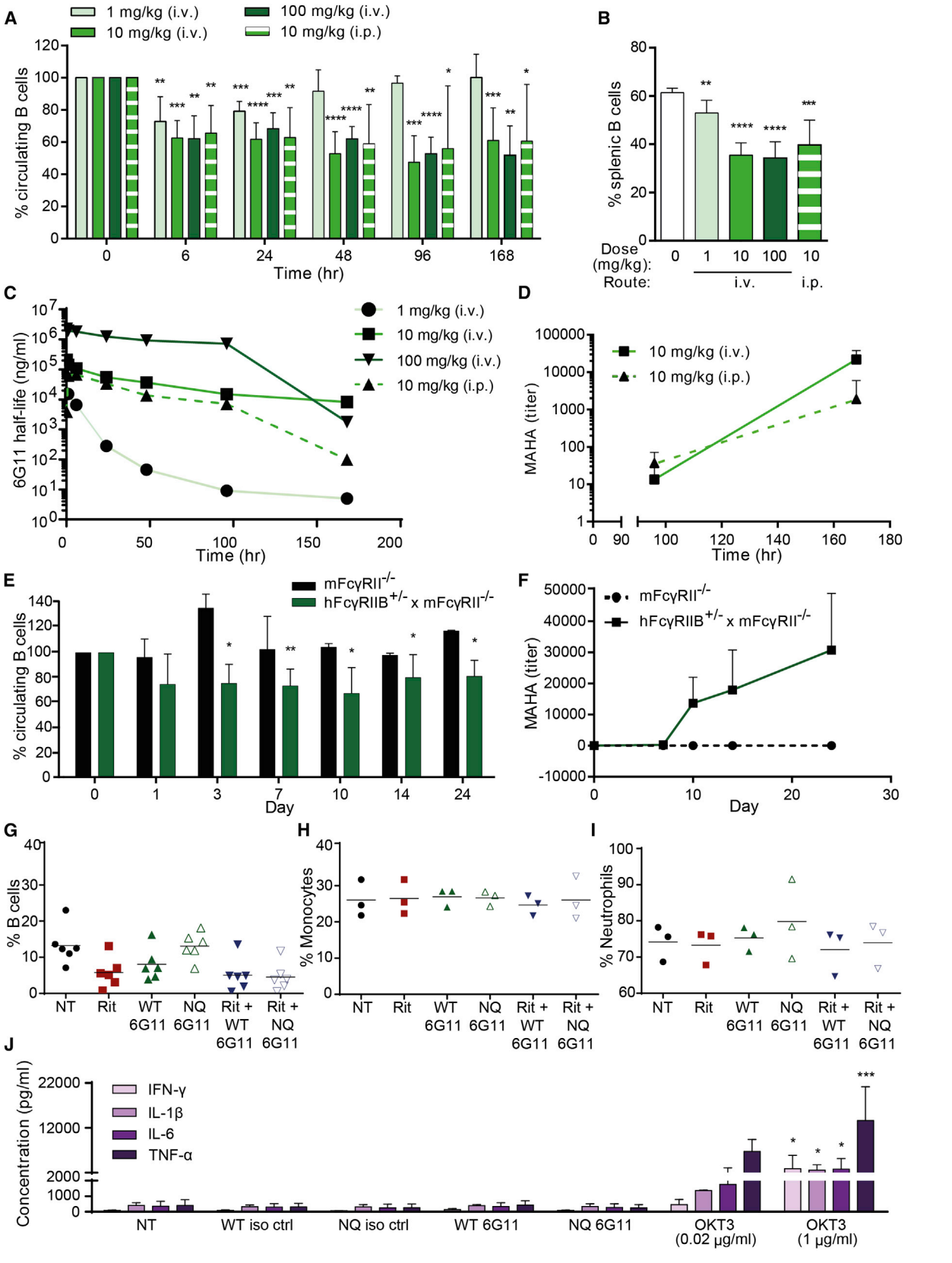


(legend on next page)

We next investigated the effect of the combination on circulatory B cells in the hCD20$^{+/-}$ × hFcγRIIB$^{+/-}$ × mFcγRII$^{-/-}$ mouse. As before, the combination resulted in significantly greater depletion of circulating B cells compared to monotherapy (Figures 5E, 5F, S5C, and S5D), demonstrating this capacity in a fully syngeneic system in which hFcγRIIB is expressed on both the target and effector cells. The effect of combining rituximab and WT hIgG1 6G11 (or AT10) was greater than that expected for additive activity (Figures 5F, left/upper, and S5D, respectively), as judged from the responses observed with the individual mAbs applied singly at 2-fold higher doses.

To assess whether intrinsic (B cell depleting) versus extrinsic (rituximab boosting) effects of 6G11 were more important for this activity, we used N297Q 6G11 in the hCD20$^{+/-}$ × hFcγRIIB$^{+/-}$ × mFcγRII$^{-/-}$ mice and show that, although N297Q 6G11 alone is inactive in deletion, it significantly boosts rituximab deletion of B cells (Figure 5F, upper). Similar results were seen with mIgG1 6G11. As expected and observed with AT10 (Figure S5D), mIgG1 6G11 displayed poor single agent depleting activity in hCD20$^{+/-}$ × hFcγRIIB$^{+/-}$ × mFcγRII$^{-/-}$ mice (Hamaguchi et al., 2006), but similar to N297Q hIgG1 6G11, was able to significantly boost a murine IgG2a version of rituximab in its ability to deplete B cells (Figure 5F, lower). Moreover, owing to its mouse Fc, it is not actively cleared by MAHAs, facilitating longer-term assessment of the combination therapy. These data show the long-term beneficial effect of antagonizing hFcγRIIB-function for enhancing rituximab's depleting activity in vivo.

Together, these studies confirmed a dual mechanism of action for 6G11 in vivo, involving intrinsic anti-tumor function coupled to the potentiation of rituximab anti-tumor activity through the prevention of internalization.

## 6G11 Boosts Rituximab-Mediated Depletion of Primary CLL Cells and Improves Objective and Complete Responses In Vivo

To better assess the anti-tumor activity of 6G11 against CLL cells, we developed a mouse model where primary human CLL cells home to lymphoid organs (spleen and bone marrow), and proliferate in clusters alongside supportive human T cells, thereby mimicking the situation in humans (Figures 6A and 6B). In this model, rituximab is highly effective at depleting CLL cells residing in the peritoneal cavity, but not the splenic proliferation centers (Figure S6A).

Mice treated with either rituximab or 6G11 alone showed significant reductions in the number of tumor cells in the spleen compared to isotype control treated mice. Whereas rituximab and 6G11 monotherapy yielded comparable results, combination therapy with rituximab and 6G11 was considerably more efficacious and statistically significant (Figures 6C and S6B and Table S3). Additionally, the numbers of objective- (OR; defined as >75% reduction of CLL cells in the spleen) and complete responders (CR; defined as <0.1% CLL cells in the spleen) following combination therapy were significantly higher than isotype control-treated mice or monotherapies (Figure 6C, bottom; Table 1). These data demonstrate the increased efficacy of the rituximab/6G11 combination therapy against primary CLL cells in vivo.

We then examined the ability of 6G11 to treat mice engrafted with CLL cells isolated from rituximab, ofatumumab (hCD20 mAb), and/or alemtuzumab (hCD52 mAb)-refractory patients (Table S4). The xenografted mice were treated with either 6G11 or rituximab as monotherapy, or with the two mAbs in combination. As expected, treatment with rituximab alone was inefficient (Figures 6D and S6C and Table S3) and >95% of mice failed to generate OR. In contrast, 6G11 alone showed significant CLL cell depletion, but failed to improve OR (Figure 6D bottom; and Table 1). Remarkably, however, co-administration of rituximab with 6G11 resulted in robust depletion (Figure 6D and Table S3) with >25% OR (Table 1). These data suggest that, in addition to boosting rituximab activity in responder patients, 6G11 may be active against treatment-refractory CLL cells.

## Combination Therapy Has Activity against MCL Cells In Vivo

To evaluate the ability of 6G11 to target other types of malignant B cells, we used immunodeficient mice engrafted with Jeko or primary MCL cells. Monotherapy with either 6G11 or rituximab did not result in long-term survival in mice engrafted with Jeko cells, whereas 30% of mice treated with the combination survived tumor-free out to 100 days (Figure S6D). Primary MCL cells also responded favorably to combination therapy (Figure S6E and Table S3).

## 6G11 Enhances Therapeutic Activity of other Clinically Relevant Antibodies In Vivo

Recent observations indicate that FcγRIIB-dependent internalization may underlie resistance to several clinically relevant antibodies besides rituximab (Vaughan et al., 2014;Pallasch et al., 2014). We therefore examined combining 6G11 with the recently approved hCD20 mAb obinutuzumab (GA101),

**Figure 4. hFcγRIIB mAb 6G11 Is Well Tolerated and Does Not Result in Toxicity**

(A–D) hFcγRIIB$^{+/-}$ × mFcγRII$^{-/-}$ mice (six to seven mice/group) were injected with 6G11. The percentage of circulating CD19$^{+}$ B220$^{+}$ B cells assessed (A, normalized to pre-dose) and the number of splenic B cells (B, expressed as the percentage of splenic lymphocytes) were quantified on day 7 whereas serum 6G11 concentrations (C) and MAHA titers (D) were assessed at the indicated times. Results are shown as mean + SD.

(E and F) hFcγRIIB$^{+/-}$ × mFcγRII$^{-/-}$ (n = 6) or mFcγRII$^{-/-}$ mice (n = 3) were injected with WT 6G11 (i.v.), followed by serial i.p. injections and circulating B cells (E) and MAHA titers (F) were assessed. Results are shown as mean ± SD. Data were analyzed using paired (A and E) and unpaired t tests (B); p values compare pre- versus post-treatment or untreated versus treated groups, respectively.

(G–I) In vitro whole blood depletion assay to assess potency of Rit ± WT or N297Q 6G11 in depleting hFcγRIIB$^{+}$ blood B cells (G), monocytes (H), or neutrophils (I). Mean values shown (horizontal lines) with each dot representing an individual donor.

(J) Cytokine response assessment using pre-cultured PBMCs left untreated (NT) or treated with WT or N297Q variants of iso ctrl or 6G11. CD3 mAb (clone OKT3) used as a positive control at optimal and sub-optimal concentrations. Supernatant cytokines assessed by MSD (mean + SD; n = 3); data analyzed using one-way ANOVA.

See also Figure S4 and Table S2.

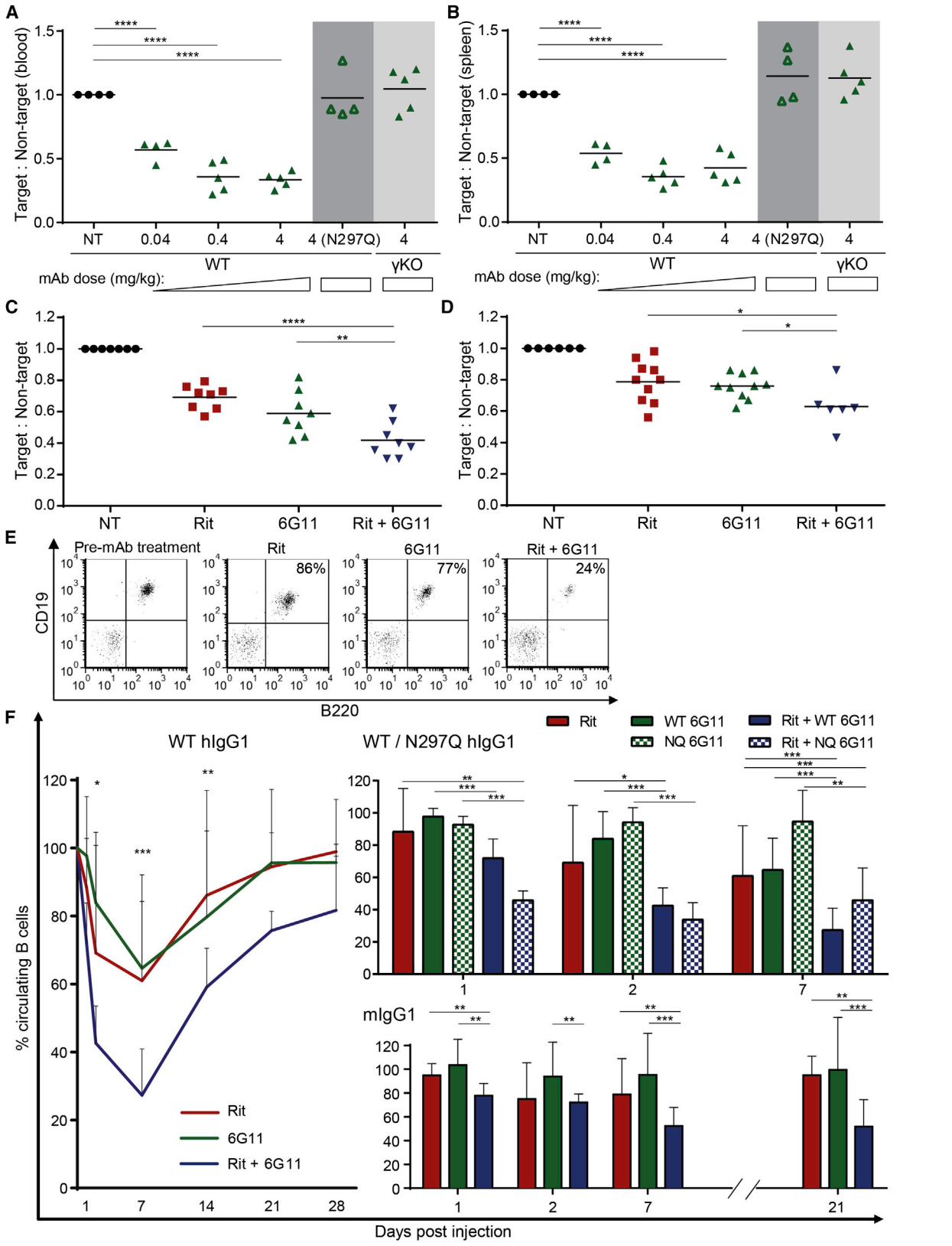


*(legend on next page)*

and the clinically well-validated hCD52 specific mAb alemtuzumab. The specificity of obinutuzumab for hCD20 allowed us to study effects in the syngeneic mouse model. Both GA101 and 6G11 monotherapy resulted in modest depletion of splenic and circulating B cells, whereas the combination significantly enhanced depletion in WT (Figures 6E and S6F) and hFcγRIIB$^{+/-}$ × mFcγRII$^{-/-}$ mice (Figures 6F and S6G). Combining 6G11 with GA101 significantly improved splenic tumor cell depletion in the CLL-patient xenograft mouse model (Figure 6G; Tables 1 and S3). Whereas alemtuzumab's specificity for hCD52 precluded studies in the syngeneic hCD20 model, there was a significant improvement in therapeutic activity when 6G11 and alemtuzumab were combined in the CLL-mouse model, with >90% of combination-treated mice developing CR (Figure 6H; Tables 1 and S3).

These data provide evidence that 6G11 may overcome mAb drug resistance for multiple targets.

## DISCUSSION

Cancer cells are highly proliferative, and genomically unstable with a high propensity for mutation, allowing drug-resistant clones to emerge after anti-cancer drug therapy, translating into treatment failure. It is now well established that tumors influence their microenvironment, subverting stromal and myeloid cells to further contribute to resistance and therapy failure (Hanahan and Weinberg, 2011). Through their ability to engage the patients' immune defense mechanisms, mAbs are important tools in contemporary cancer therapy (Weiner et al., 2010) and comprise a rapidly expanding class of drugs. Since the approval of rituximab in 1997, and the recent approval of ofatumumab and obinutuzumab (Lim et al., 2010), these agents have become central to the armamentarium for treating cancer. However, it is clear that mAb immunotherapy is also susceptible to both intrinsic and acquired resistance (Bardelli and Siena, 2010; Montagut et al., 2012; Rampias et al., 2014; Rezvani and Maloney, 2011; Wong and Lee, 2012).

At least two mechanisms of resistance, which may affect numerous therapeutic mAbs, are precipitated by the inhibitory FcγRIIB (Williams et al., 2013a). In addition to the inhibitory effect on effector cells (Clynes et al., 2000), rituximab and other type I hCD20 mAbs engage hFcγRIIB by bipolar antibody bridging on the B cell surface, resulting in internalization of the mAb:CD20:FcγRIIB complex (Lim et al., 2011; Vaughan et al., 2014), limiting its ability to engage key Fc-dependent effector functions. This mechanism is relevant for several different targets, because mAbs to other surface receptors are also internalized in an hFcγRIIB-dependent manner (Pallasch et al., 2014; Vaughan et al., 2014). Here, we describe the generation of fully human hFcγRIIB mAbs that are able to block both of these resistance mechanisms and are thus able to unleash the full potential of other therapeutic mAbs and help overcome resistance to mAb therapy in vivo.

Co-administration of hFcγRIIB mAb did not only improve OR and CR responses in mice engrafted with CLL cells from patients with rituximab-responsive disease, but also overcame the mAb treatment-resistant phenotype of CLL cells from patients with relapsed/refractory disease resistant to rituximab, ofatumumab, or alemtuzumab. A role for tumor cell FcγRIIB was recently proposed in resistance to hCD52 mAb therapy in select microenvironments (Pallasch et al., 2014). hFcγRIIB was upregulated in alemtuzumab-resistant bone marrow leukemic B cells compared with more susceptible splenic compartments, and shRNA-mediated knock-down of hFcγRIIB in these cells improved hCD52 mAb therapy in otherwise resistant tissue. These findings are consistent with the observations made in our CLL model. Whereas CLL cells in susceptible peritoneal compartments were readily depleted by hCD20 mAb, depletion in resistant microenvironments required blocking of tumor FcγRIIB. Consistent with high FcγRIIB expression underlying decreased mAb activity in resistant tissue compartments, FcγRIIB-blocking enhanced alemtuzumab and also type II hCD20 mAb in our CLL model. We previously showed that type II hCD20 mAbs only internalize efficiently in the presence of high levels of FcγRIIB (Vaughan et al., 2014). Collectively, these observations demonstrate that FcγRIIB-mediated resistance is relevant to several different clinically approved antibodies, indicating a broad therapeutic potential for combination with hFcγRIIB mAb.

FcγRIIB-mAb combination was also relevant to different tumor types, with co-administration of 6G11 boosting rituximab antitumor activity in both CLL and MCL models in vivo. These findings provide in vivo-proof-of-concept and solidify our previous observations (Lim et al., 2011) identifying FcγRIIB-mediated

**Figure 5. hFcγRIIB mAb 6G11 Is Active In Vivo and Potentiates CD20 mAb Depletion of B Cells**

(A and B) hFcγRIIB$^{+/-}$ × mFcγRII$^{-/-}$ target and mFcγRII$^{-/-}$ non-target splenocytes labeled with high or low levels of CFSE, respectively, were adoptively transferred into WT or γKO recipient mice. Mice received WT or N297Q (NQ) 6G11, as indicated, and circulating (A) or splenic (B) cells were analyzed to determine the ratio of CD19$^{+}$ target: non-target cells remaining; normalized to ctrl group (NT) given a ratio of 1.0. Data combined from at least two independent experiments.

(C) CSFE$^{+}$ hCD20$^{+/-}$ × hFcγRIIB$^{+/-}$ × mFcγRII$^{-/-}$ (target) and mFcγRII$^{-/-}$ (non-target) splenocytes were injected (i.v.) into WT recipient mice and injected with mAbs alone or in combination (0.2–0.4 mg/kg). Spleens were analyzed as above. Data combined from at least three independent experiments.

(D) CFSE$^{+}$ hCD20$^{+/-}$ × hFcγRIIB$^{+/-}$ × mFcγRII$^{-/-}$ (target) and mFcγRII$^{-/-}$ (non-target) splenocytes were injected into hFcγRIIB$^{+/-}$ × mFcγRII$^{-/-}$ recipient mice. Mice received WT 6G11 (2 × 20 mg/kg) followed by Rit (0.2–2 mg/kg) and the ratio of splenic CD19$^{+}$ cells determined, as above. Data combined from at least three independent experiments.

(A–D) Each dot depicts a result from an individual mouse, with mean ratios indicated by the horizontal line. One-way ANOVA performed.

(E and F) hCD20$^{+/-}$ × hFcγRIIB$^{+/-}$ × mFcγRII$^{-/-}$ mice received either Rit ± WT or N297Q 6G11 (20 mg/kg) or 10 mg/kg of each mAb in combination on day 0 and the number of circulating B cells assessed over time. (E) Representative dot plots analyzing circulatory B cells indicating pre-treatment and day 2 post-mAb injection. Numbers in the upper right quadrants indicate percent B cells compared to pre-treatment levels. (F) Left graph indicating depletion of circulating B cells with Rit ± WT 6G11; top right graph indicates depletion of circulating B cells with Rit ± WT or N297Q 6G11; lower right graph indicates depletion of circulating B cells with Rit (m2a; 4 mg/kg) ± 6G11 (mIgG1; 20 mg/kg). Means + SD of percent circulating B cells post-treatment, normalized to pre-treatment levels, shown; up to 12 mice/group combined from at least two independent experiments. Two-way ANOVA performed.

See also Figure S5.

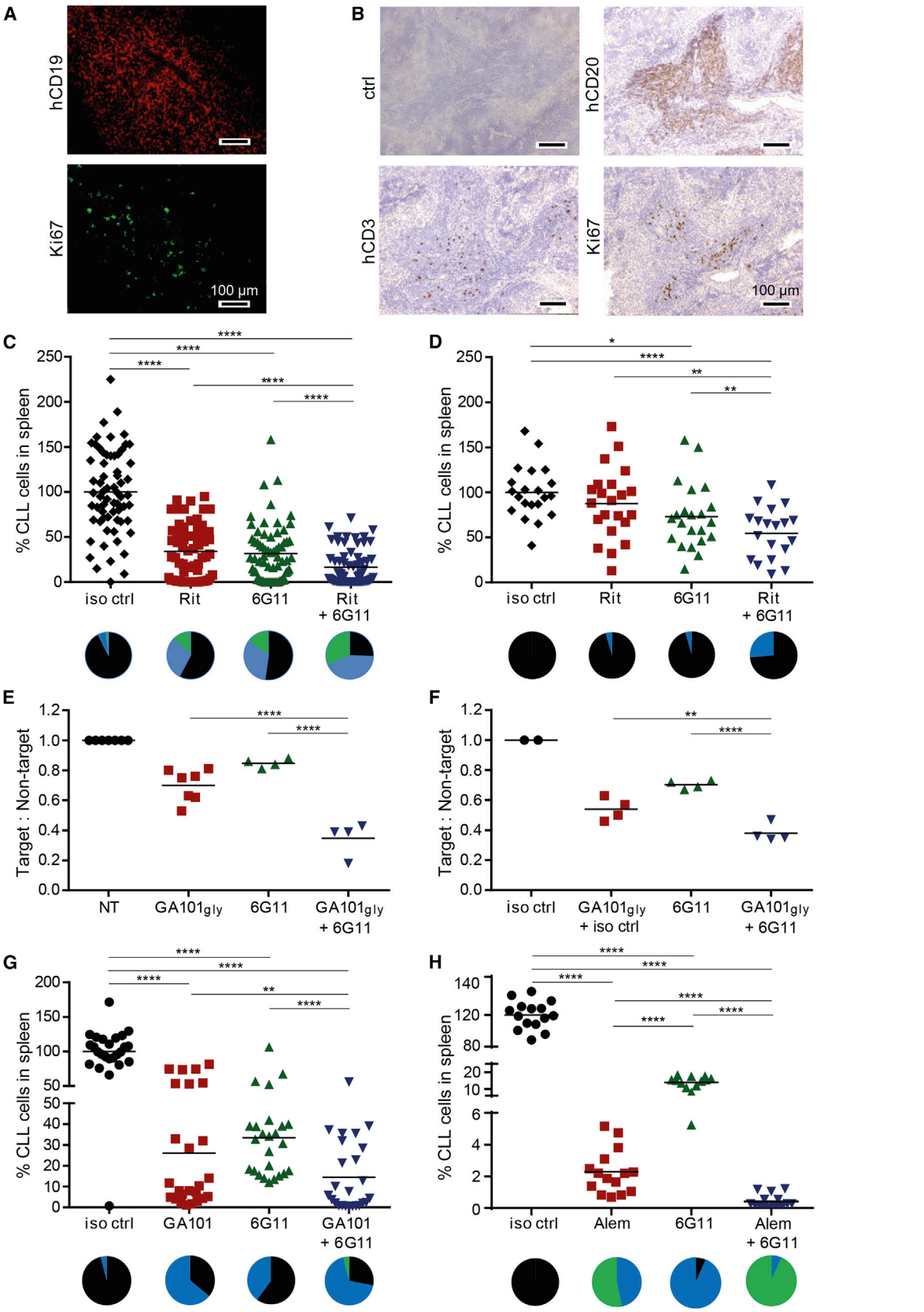


*(legend on next page)*

mAb internalization as a common mechanism underlying resistance in different B cell cancers and individuals.

Considering additional potential mechanisms of action, we demonstrate that hFcγRIIB mAbs have intrinsic anti-tumor activity. Veri et al. previously developed hFcγRIIB-specific mAbs but did not examine their activity against cancer targets in vivo (Veri et al., 2007). Rankin et al. subsequently showed that targeting hFcγRIIB on malignant human B cell lines could be efficacious as a monotherapy. However, this study (Rankin et al., 2006) used xenograft systems, where the target antigen was expressed only on the tumor, and not critical immune effectors, precluding assessment of the net effects of hFcγRIIB mAb. In the current work, using two different mAbs (6G11 and AT10), we demonstrate in immunocompetent syngeneic mouse models where hFcγRIIB is expressed on both the target B cells and effectors, that antagonistic hFcγRIIB mAbs have intrinsic target cell depleting activity.

At least three distinct mechanisms may thus contribute to the overall in vivo therapeutic activity of 6G11: intrinsic cytotoxicity, prevention of therapeutic mAb internalization, and neutralization of FcγRIIB-inhibitory signaling in immune cells. Several observations suggest that blocking receptor internalization and inhibitory signaling are the most critical for overcoming drug resistance. First, there was a pronounced and apparently synergistic effect when antagonistic hFcγRIIB and hCD20 mAbs were co-administrated to the mice where hFcγRIIB is expressed on both target and effector cells. Second, we found that whereas B cell deletion was inefficient with AT10 alone, the combination of AT10 and rituximab was effective in augmenting rituximab activity. Most definitively, our data with N297Q hIgG1 6G11, which lacks the ability to engage activatory FcγR and has no direct cytotoxic capacity, confirms that blocking FcγRIIB activity is the key mechanism behind the efficacy of this approach. This provides evidence that function-blocking mAbs to FcγRIIB can recapitulate the enhanced anti-cancer mAb responses observed following genetic deletion of FcγRIIB (Clynes et al., 2000). However, here we have not explored directly the relative importance of antagonizing FcγRIIB function on the target versus immune effector cells for activity; these studies form the basis of our ongoing endeavors.

Of note, it has long been appreciated that CLL is sub-optimally treated with rituximab (O'Brien et al., 2001) and ofatumumab (Coiffier et al., 2006, 2008) with higher doses being required. Coupled to our previous data, our current results indicate that combination therapy with hFcγRIIB mAb may not only be a way of preventing resistance, but perhaps also of decreasing the dose or shortening duration of hCD20 mAb therapy.

In addition to affording significant activity, a therapeutic mAb must be tolerable and have therapeutically relevant PK. The high specificity of 6G11 for hFcγRIIB, with its lack of binding to hFcγRIIA, and negligible cross-reactivity with animal species commonly used for toxicological studies, prompted us to investigate safety parameters and PK/pharmacodynamics (PD) in mice expressing hFcγRIIB at levels and on cell types and tissues similar to those of humans. These studies indicated that 6G11 was well tolerated with a therapeutically relevant PK profile typical for a hIgG1 mAb with an estimated half-life of weeks in man.

Interestingly, in both human blood and in vivo in hFcγRIIB Tg mice, 6G11 treatment resulted in specific deletion of B cells. Although monocytes in both systems express hFcγRIIB, they were not substantially deleted. Current evidence suggests that macrophages and/or monocytes are the key effector cells responsible for mAb therapy (Beers et al., 2010; Biburger et al., 2011; Gül et al., 2014) and so our data indicate that the key effectors are not deleted by hFcγRIIB mAb.

We previously explored an equivalent panel of mFcγRII-specific mAbs (Williams et al., 2012) and observed that they had limited therapeutic benefit due to their rapid consumption in vivo (Williams et al., 2013b). Similar rates of internalization were not seen on human target cells, at least in vitro, in agreement with earlier studies (Rankin et al., 2006). Here, we extended these observations and demonstrated that on primary human CLL samples and in mice expressing hFcγRIIB, rapid and extensive mAb consumption was not observed. These data confirm our earlier supposition that mouse and human inhibitory FcγRIIB have different properties in relation to their capacity for internalization and to function as an antigenic sink, and support that hFcγRIIB is a pharmacodynamically and therapeutically relevant target in humans.

Collectively, our results demonstrate in vivo proof-of-concept that hFcγRIIB mAbs overcome the intrinsic and acquired resistance of tumor cells to mAb drugs, and can restore responsiveness to mAb therapy in relapsed/refractory tumors. These data support the clinical development of hFcγRIIB mAbs for therapy of FcγRIIB-expressing B cell cancers. Furthermore, analogous to the spread of CD20 mAbs into other diseases, there is evidence to suggest their utility in other therapeutic settings such

**Figure 6. hFcγRIIB mAb 6G11 Potentiates Therapeutic mAb Depletion of Normal and Malignant Target Cells In Vivo**

(A and B) The spleen of a NOD/SCID mouse engrafted with primary CLL cells from a patient was assessed by immunofluorescence (A) or by IHC (B); ctrl, no primary mAb.

(C) Mice xenografted with human CLL cells (n = 11 patients) were treated with 1–10 mg/kg of hCD20 mAb (Rit), hFcγRIIB mAb (6G11), or both and percent CLL cells remaining in the spleen enumerated and normalized to the proportion after treatment with iso ctrl.

(D) Mice xenografted with CLL cells from patients previously designated as refractory (n = 4 patients) were treated and assessed as in (C).

(E) $CFSE^{+}$ $hCD20^{+/-}$ × $hFc\gamma RIIB^{+/-}$ × $mFc\gamma RII^{-/-}$ (target) and $mFc\gamma RII^{-/-}$ (non-target) splenocytes were injected (i.v.) into WT mice and treated with $GA101_{gly}$ or 6G11 alone or in combination (0.008 mg/kg) and assessed for deletion in the spleen as before. Data combined from two to three independent experiments.

(F) $CFSE^{+}$ $hCD20^{+/-}$ × $hFc\gamma RIIB^{+/-}$ × $mFc\gamma RII^{-/-}$ (target) and $mFc\gamma RII^{-/-}$ (non-target) splenocytes were injected into $hFc\gamma RIIB^{+/-}$ × $mFc\gamma RII^{-/-}$ recipient mice and treated with either WT iso ctrl or 6G11 (20 mg/kg), followed by $GA101_{gly}$ (0.04 mg/kg) and analyzed as in (E).

(G) Mice engrafted with CLL cells (n = 4 patients) were treated with GA101 (0.2 mg/kg), 6G11 (1 mg/kg), or both and assessed as in (C).

(H) Mice engrafted with CLL cells (n = 3 patients) were treated with alemtuzumab (Alem; 1 mg/kg), 6G11 (1 mg/kg), or both and assessed as in (C). (C, D, G, and H) Pie charts represent the number of NR (black), OR (blue), and CR (green) primary patient CLL-bearing mice following mAb therapy, as defined in Table 1.

(C–H) Each dot depicts an individual mouse, with mean ratios indicated by the horizontal line. (E and F) Data analyzed using one-way ANOVA and (C, D, G, and H) a permutation statistical test. See also Figure S6 and Tables S3 and S4.

**Table 1. Reponses to mAb Treatment in Primary CLL-Patient Xenografts**

| Therapeutic mAb (samples) | Treatment No. of CLL Samples | Isotype ctrl, % (n/N) | | | Therapeutic mAb, % (n/N) | | | 6G11 (hFcγRIIB), % (n/N) | | | Therapeutic mAb + 6G11, % (n/N) | | |
|---|---|---|---|---|---|---|---|---|---|---|---|---|---|
| | | NR | OR | CR | NR | OR | CR | NR | OR | CR | NR | OR | CR |
| Rituximab (all-comers) | 11 | 94 (61/65) | 4.5 (3/65) | 1.5 (1/65) | 58 (37/64) | 30[a] (19/64) | 12[b] (8/64) | 52 (35/67) | 33[a] (22/67) | 15[c] (10/67) | 26 (17/66) | 42[a,d,f] (28/66) | 32[a,e,f] (21/66) |
| Rituximab (refractory) | 4 | 100 (21/21) | 0 | 0 | 95.5 (21/22) | 4.5 (1/22) | 0 | 95.5 (21/22) | 4.5 (1/22) | 0 | 74 (14/19) | 26[c] (5/19) | 0 |
| GA101 (all-comers) | 3 | 100 (20/20) | 0 | 0 | 30 (6/20) | 70[a] (14/20) | 0 | 50 (10/20) | 50[a] (10/20) | 0 | 20 (4/20) | 75[a] (15/20) | 5 (1/20) |
| GA101 (resistant) | 1 | 80 (4/5) | 20 (1/5) | 0 | 80 (4/5) | 20 (1/5) | 0 | 100 (5/5) | 0 | 0 | 40 (2/5) | 60 (3/5) | 0 |
| Alemtuzumab (all-comers) | 3 | 100 (15/15) | 0 | 0 | 0 | 47[b] (7/15) | 53[b] (8/15) | 7 (1/14) | 93[a] (13/14) | 0 | 0 | 7 (1/15) | 93[a,d,e] (14/15) |

All-comers, primary CLL samples with no indication of prior resistance; resistant, primary CLL samples with prior demonstration of rituximab resistance; NR, non-responder (no CLL cell depletion); OR, objective responder (≥75% reduction in CLL cells); CR, complete responder (≤0.1% CLL cells).
[a] $p \leq 0.001$ vs isotype control.
[b] $p \leq 0.05$ vs isotype control.
[c] $p \leq 0.01$ vs isotype control.
[d] $p \leq 0.001$ vs therapeutic mAb.
[e] $p \leq 0.05$ vs therapeutic mAb.
[f] $p \leq 0.01$ vs therapeutic mAb.

as autoimmunity where FcγRIIB-expressing targets may be amenable to manipulation, for example in systemic light-chain amyloidosis where the target PCs express high levels of FcγRIIB (Zhou et al., 2008) and rheumatoid arthritis where B cell activation might be reduced through agonism of FcγRIIB (Baerenwaldt et al., 2011; Mauri and Jury, 2010). Clinical investigations in all of these areas are now warranted. We aim to develop this approach as a first-in-human clinical trial in combination with rituximab in non-Hodgkin lymphoma patients later this year.

## EXPERIMENTAL PROCEDURES

### Animals

Human (h) CD20 Tg, γ-chain$^{-/-}$ and mouse (m) FcγRIIB$^{-/-}$ mice have been described previously (Beers et al., 2008) with genotypes confirmed by PCR and/or flow cytometry. CB-17 SCID and NOD/SCID mice were purchased from Charles River and Taconic, respectively and then bred and maintained in local animal facilities. Mice were bred and maintained in local facilities in accordance with the UK Home Office and Swedish Board of Agriculture guidelines. Animal experiments were regulated through local ethical committees and were performed under Home Office licenses (PPL30/1269 and M90-11) and BioInvent general permit allowing animal work (31-11587/10).

### Clinical Samples and Ethics

Ethical approval for the use of clinical samples was obtained by the Southampton University Hospitals NHS Trust from the Southampton and South West Hampshire Research Ethics Committee or by the Ethics Committee of Skåne University Hospital. Informed consent was provided in accordance with the Declaration of Helsinki. Samples were released from the Human Tissue Authority licensed University of Southampton, Cancer Science Unit Tissue Bank or obtained through the Department of Hematology and Department of Oncology at Skånes University Hospital, Lund.

### Generation of hFcγRIIB mAb

hFcγRIIB mAbs were identified by screening the n-CoDeR scFv phage display library using the extracellular domain of hFcγRIIB and hFcγRIIA fused to mIgG3-Fc (hFcγRIIB/A-Fc) as target and non-target, respectively. Full details in are provided in the Supplemental Experimental Procedures.

### Immunotherapy In Vivo

#### *Subcutaneous Models*

Daudi ($5 \times 10^6$) were injected subcutaneously with growth factor reduced Matrigel (BD Biosciences) into SCID mice and subsequently treated with mAb on days 7, 14, 21, and 28. Tumor growth was calculated as [weight (mg) = (length × width$^2$)/2].

#### *Adoptive Transfer*

This procedure was performed as detailed elsewhere (Beers et al., 2010) and in the Supplemental Experimental Procedures.

#### *B Cell Depletion*

Mice were given hCD20 or hFcγRIIB mAbs alone or in combination intravenously (i.v.) and leukocytes were assessed as described elsewhere (Beers et al., 2010).

#### *Primary Human Xenograft Models*

Patients' PBMCs were isolated and injected ($6–10 \times 10^7$ cells) i.v. into irradiated (1 Gy) mice. Four to five days later, mice were treated with mAbs (intraperitoneally [i.p.]), with a second injection 2–3 days later and killed 2–3 days after that. Spleens were harvested, and human cells were identified and quantified as CD45$^+$ CD5$^+$ CD19$^+$.

### PD, PK, and Immunogenicity Studies

hFcγRIIB$^{+/-}$ × mFcγRII$^{-/-}$ mice were injected with a single dose of WT 6G11 i.v. or i.p. or with multiple shots of 10 mg/kg. Mice were examined throughout for signs of distress, weight loss, B cell numbers (CD19$^+$ B220$^+$), toxicity, or pathology. Serum concentrations of 6G11 and MAHA were determined as described in the Supplemental Experimental Procedures.

### Statistical Analysis

To compare experimental groups, Wilcoxon, paired or unpaired t test analyses were performed; Kaplan Meier curves were produced and analyzed by Log rank test. For in vivo adoptive transfer assays containing more than two groups, one- or two-way ANOVA were used. To evaluate the efficacy of mAbs in the in vivo xenograft experiments, the percentages of tumor cells in the spleens of treated animals were measured and the average difference in percentage between animals xenografted with tumor cells from the same patient were calculated. These differences were then averaged across patients to obtain a summary statistic that reflects the overall effect. To calculate the distribution of this statistical test under the null hypothesis, we used a permutation approach where test group labels were randomly reassigned within patients. One billion permutations were used. This approach does not make any parametric or other distributional assumptions and ensures a p value resolution of $1 \times 10^{-9}$. As a complement to this approach, we used standard parametric tests (one-way ANOVA), which yielded similar results. For differences in OR and CR, Chi-square tests were used. Statistical analysis was performed using GraphPadPrism (v5 or 6). Stars denote significance as follows: *$p \leq 0.05$, **$p \leq 0.01$, ***$p \leq 0.001$, and ****$p \leq 0.0001$, unless otherwise stated.

## SUPPLEMENTAL INFORMATION

Supplemental Information includes Supplemental Experimental Procedures, six figures, and four tables and can be found with this article online at http://dx.doi.org/10.1016/j.ccell.2015.03.005.

## AUTHOR CONTRIBUTIONS

A.R. and I.T. performed research, analyzed and interpreted data, and helped write the manuscript; L.M., K.L.C., M.K., A.L., J.M., A.S., A.T.V, V.S., N.S, B.S., H.T.C., Z.L., E.L.W., G.M, R.J.O., C.I.M., S.A.J., L.N.D., K.H., and B.N. all generated or provided key reagents or performed and analyzed research; J.S.V., G.J., M.H., and M.J. contributed key reagents and to discussion of the data; A.D., S.A.B., P.W.M.J., and M.J.G. discussed and interpreted data and edited the manuscript; B.F. and M.S.C. designed the study, analyzed and interpreted data, and wrote the manuscript.

## ACKNOWLEDGMENTS

We are grateful to all patients and volunteers who generously donated their biological specimens for research, and Drs. F. Forconi, A. Duncombe, K. Potter, A. Steele, I. Tracy, and I. Wheatley for provision and assistance with clinical material. We would like to thank colleagues from the Cancer Sciences Unit who provided advice and technical support, including A. Tutt, R. French, C. Lee; P. Duriez (Protein Core Facility) for production of recombinant M-CSF; and the Biomedical Research Facility for animal husbandry. Funding was provided by Leukaemia and Lymphoma Research grants 08014, 08048, 09009, and 12009; and CRUK grants C1477/A10834 and C34999/A18087.

I.T., B.F., L.M., M.K., A.L., J.M., A.S., and Z.L. are or were employees of BioInvent International during their contribution to this paper. G.M. received funding from BioInvent. M.S.C. acts as a consultant to BioInvent and Roche and has received institutional support from BioInvent for grants and patents. M.J.G. receives an institutional grant from Cancer Research UK, acts as a consultant to a number of biotech companies to write general antibody expert reports, and receives institutional payments and royalties from antibody patents and licenses. P.W.M.J. acts as a consultant to Roche and Pfizer and has received payments for lectures from Millennium Takeda and Pfizer.

Received: June 27, 2014
Revised: November 19, 2014
Accepted: March 10, 2015
Published: April 13, 2015

## REFERENCES

Baerenwaldt, A., Lux, A., Danzer, H., Spriewald, B.M., Ullrich, E., Heidkamp, G., Dudziak, D., and Nimmerjahn, F. (2011). Fcγ receptor IIB (FcγRIIB) maintains humoral tolerance in the human immune system in vivo. Proc. Natl. Acad. Sci. USA *108*, 18772–18777.

Bardelli, A., and Siena, S. (2010). Molecular mechanisms of resistance to cetuximab and panitumumab in colorectal cancer. J. Clin. Oncol. *28*, 1254–1261.

Beers, S.A., Chan, C.H., James, S., French, R.R., Attfield, K.E., Brennan, C.M., Ahuja, A., Shlomchik, M.J., Cragg, M.S., and Glennie, M.J. (2008). Type II (tositumomab) anti-CD20 monoclonal antibody out performs type I (rituximab-like) reagents in B-cell depletion regardless of complement activation. Blood *112*, 4170–4177.

Beers, S.A., French, R.R., Chan, H.T., Lim, S.H., Jarrett, T.C., Vidal, R.M., Wijayaweera, S.S., Dixon, S.V., Kim, H., Cox, K.L., et al. (2010). Antigenic modulation limits the efficacy of anti-CD20 antibodies: implications for antibody selection. Blood *115*, 5191–5201.

Biburger, M., Aschermann, S., Schwab, I., Lux, A., Albert, H., Danzer, H., Woigk, M., Dudziak, D., and Nimmerjahn, F. (2011). Monocyte subsets responsible for immunoglobulin G-dependent effector functions in vivo. Immunity *35*, 932–944.

Cartron, G., Dacheux, L., Salles, G., Solal-Celigny, P., Bardos, P., Colombat, P., and Watier, H. (2002). Therapeutic activity of humanized anti-CD20 monoclonal antibody and polymorphism in IgG Fc receptor FcgammaRIIIa gene. Blood *99*, 754–758.

Clynes, R.A., Towers, T.L., Presta, L.G., and Ravetch, J.V. (2000). Inhibitory Fc receptors modulate in vivo cytotoxicity against tumor targets. Nat. Med. *6*, 443–446.

Coiffier, B., Tilly, H., Pedersen, L.M., Plesner, T., Frederiksen, H., van Oers, M.H.J., Wooldridge, J., Kloczko, J.S., Holowiecki, J., Hellmann, A., et al. (2006). Significant correlation between survival endpoints and exposure to ofatumumab (HuMax-CD20) in chronic lymphocytic leukemia. Blood *108*, 2842.

Coiffier, B., Lepretre, S., Pedersen, L.M., Gadeberg, O., Fredriksen, H., van Oers, M.H., Wooldridge, J., Kloczko, J., Holowiecki, J., Hellmann, A., et al. (2008). Safety and efficacy of ofatumumab, a fully human monoclonal anti-CD20 antibody, in patients with relapsed or refractory B-cell chronic lymphocytic leukemia: a phase 1-2 study. Blood *111*, 1094–1100.

Cragg, M.S., Morgan, S.M., Chan, H.T., Morgan, B.P., Filatov, A.V., Johnson, P.W., French, R.R., and Glennie, M.J. (2003). Complement-mediated lysis by anti-CD20 mAb correlates with segregation into lipid rafts. Blood *101*, 1045–1052.

Dyer, M.J., Hale, G., Hayhoe, F.G., and Waldmann, H. (1989). Effects of CAMPATH-1 antibodies in vivo in patients with lymphoid malignancies: influence of antibody isotype. Blood *73*, 1431–1439.

Greenman, J., Tutt, A.L., George, A.J., Pulford, K.A., Stevenson, G.T., and Glennie, M.J. (1991). Characterization of a new monoclonal anti-Fc gamma RII antibody, AT10, and its incorporation into a bispecific F(ab')2 derivative for recruitment of cytotoxic effectors. Mol. Immunol. *28*, 1243–1254.

Gül, N., Babes, L., Siegmund, K., Korthouwer, R., Bögels, M., Braster, R., Vidarsson, G., ten Hagen, T.L., Kubes, P., and van Egmond, M. (2014). Macrophages eliminate circulating tumor cells after monoclonal antibody therapy. J. Clin. Invest. *124*, 812–823.

Hamaguchi, Y., Xiu, Y., Komura, K., Nimmerjahn, F., and Tedder, T.F. (2006). Antibody isotype-specific engagement of Fcgamma receptors regulates B lymphocyte depletion during CD20 immunotherapy. J. Exp. Med. *203*, 743–753.

Hanahan, D., and Weinberg, R.A. (2011). Hallmarks of cancer: the next generation. Cell *144*, 646–674.

Hussain, K., Hargreaves, C.E., Roghanian, A., Oldham, R.J., Chan, H.T., Mockridge, C.I., Chowdhury, F., Frendéus, B., Harper, K.S., Strefford, J.C., et al. (2015). Upregulation of FcγRIIb on monocytes is necessary to promote the superagonist activity of TGN1412. Blood *125*, 102–110.

Lee, C.S., Ashton-Key, M., Cogliatti, S., Rondeau, S., Schmitz, S.F., Ghielmini, M., Cragg, M.S., and Johnson, P. (2015). Expression of the inhibitory Fc gamma receptor IIB (FCGR2B, CD32B) on follicular lymphoma cells lowers the response rate to rituximab monotherapy (SAKK 35/98). Br. J. Haematol. *168*, 145–148.

Lim, S.H., Beers, S.A., French, R.R., Johnson, P.W., Glennie, M.J., and Cragg, M.S. (2010). Anti-CD20 monoclonal antibodies: historical and future perspectives. Haematologica *95*, 135–143.

Lim, S.H., Vaughan, A.T., Ashton-Key, M., Williams, E.L., Dixon, S.V., Chan, H.T., Beers, S.A., French, R.R., Cox, K.L., Davies, A.J., et al. (2011). Fc gamma receptor IIb on target B cells promotes rituximab internalization and reduces clinical efficacy. Blood *118*, 2530–2540.

Mauri, C., and Jury, E.C. (2010). Could the expression of CD86 and FcγRIIB on B cells be functionally related and involved in driving rheumatoid arthritis? Arthritis Res. Ther. *12*, 133.

Minard-Colin, V., Xiu, Y., Poe, J.C., Horikawa, M., Magro, C.M., Hamaguchi, Y., Haas, K.M., and Tedder, T.F. (2008). Lymphoma depletion during CD20 immunotherapy in mice is mediated by macrophage FcgammaRI, FcgammaRIII, and FcgammaRIV. Blood *112*, 1205–1213.

Montagut, C., Dalmases, A., Bellosillo, B., Crespo, M., Pairet, S., Iglesias, M., Salido, M., Gallen, M., Marsters, S., Tsai, S.P., et al. (2012). Identification of a mutation in the extracellular domain of the Epidermal Growth Factor Receptor conferring cetuximab resistance in colorectal cancer. Nat. Med. *18*, 221–223.

Montalvao, F., Garcia, Z., Celli, S., Breart, B., Deguine, J., Van Rooijen, N., and Bousso, P. (2013). The mechanism of anti-CD20-mediated B cell depletion revealed by intravital imaging. J. Clin. Invest. *123*, 5098–5103.

Nimmerjahn, F., and Ravetch, J.V. (2008). Fcgamma receptors as regulators of immune responses. Nat. Rev. Immunol. *8*, 34–47.

Nimmerjahn, F., and Ravetch, J.V. (2011). FcγRs in health and disease. Curr. Top. Microbiol. Immunol. *350*, 105–125.

O'Brien, S.M., Kantarjian, H., Thomas, D.A., Giles, F.J., Freireich, E.J., Cortes, J., Lerner, S., and Keating, M.J. (2001). Rituximab dose-escalation trial in chronic lymphocytic leukemia. J. Clin. Oncol. *19*, 2165–2170.

Pallasch, C.P., Leskov, I., Braun, C.J., Vorholt, D., Drake, A., Soto-Feliciano, Y.M., Bent, E.H., Schwamb, J., Iliopoulou, B., Kutsch, N., et al. (2014). Sensitizing protective tumor microenvironments to antibody-mediated therapy. Cell *156*, 590–602.

Rampias, T., Giagini, A., Siolos, S., Matsuzaki, H., Sasaki, C., Scorilas, A., and Psyrri, A. (2014). RAS/PI3K crosstalk and cetuximab resistance in head and neck squamous cell carcinoma. Clin. Cancer Res *20*, 2933–2946.

Rankin, C.T., Veri, M.C., Gorlatov, S., Tuaillon, N., Burke, S., Huang, L., Inzunza, H.D., Li, H., Thomas, S., Johnson, S., et al. (2006). CD32B, the human inhibitory Fc-gamma receptor IIB, as a target for monoclonal antibody therapy of B-cell lymphoma. Blood *108*, 2384–2391.

Ravetch, J.V., and Perussia, B. (1989). Alternative membrane forms of Fc gamma RIII(CD16) on human natural killer cells and neutrophils. Cell type-specific expression of two genes that differ in single nucleotide substitutions. J. Exp. Med. *170*, 481–497.

Reichert, J.M., and Dhimolea, E. (2012). The future of antibodies as cancer drugs. Drug Discov. Today *17*, 954–963.

Rezvani, A.R., and Maloney, D.G. (2011). Rituximab resistance. Best Pract. Res. Clin. Haematol. *24*, 203–216.

Römer, P.S., Berr, S., Avota, E., Na, S.Y., Battaglia, M., ten Berge, I., Einsele, H., and Hünig, T. (2011). Preculture of PBMCs at high cell density increases sensitivity of T-cell responses, revealing cytokine release by CD28 superagonist TGN1412. Blood *118*, 6772–6782.

Söderlind, E., Strandberg, L., Jirholt, P., Kobayashi, N., Alexeiva, V., Aberg, A.M., Nilsson, A., Jansson, B., Ohlin, M., Wingren, C., et al. (2000). Recombining germline-derived CDR sequences for creating diverse single-framework antibody libraries. Nat. Biotechnol. *18*, 852–856.

Tao, M.H., and Morrison, S.L. (1989). Studies of aglycosylated chimeric mouse-human IgG. Role of carbohydrate in the structure and effector functions mediated by the human IgG constant region. J. Immunol. *143*, 2595–2601.

Vaughan, A.T., Iriyama, C., Beers, S.A., Chan, C.H., Lim, S.H., Williams, E.L., Shah, V., Roghanian, A., Frendéus, B., Glennie, M.J., and Cragg, M.S. (2014). Inhibitory FcγRIIb (CD32b) becomes activated by therapeutic mAb in both cis and trans and drives internalization according to antibody specificity. Blood *123*, 669–677.

Veri, M.C., Gorlatov, S., Li, H., Burke, S., Johnson, S., Stavenhagen, J., Stein, K.E., Bonvini, E., and Koenig, S. (2007). Monoclonal antibodies capable of discriminating the human inhibitory Fcgamma-receptor IIB (CD32B) from the activating Fcgamma-receptor IIA (CD32A): biochemical, biological and functional characterization. Immunology *121*, 392–404.

Weiner, L.M., Surana, R., and Wang, S. (2010). Monoclonal antibodies: versatile platforms for cancer immunotherapy. Nat. Rev. Immunol. *10*, 317–327.

Weng, W.K., and Levy, R. (2003). Two immunoglobulin G fragment C receptor polymorphisms independently predict response to rituximab in patients with follicular lymphoma. J. Clin. Oncol. *21*, 3940–3947.

Williams, E.L., Tutt, A.L., French, R.R., Chan, H.T., Lau, B., Penfold, C.A., Mockridge, C.I., Roghanian, A., Cox, K.L., Verbeek, J.S., et al. (2012). Development and characterisation of monoclonal antibodies specific for the murine inhibitory FcγRIIB (CD32B). Eur. J. Immunol. *42*, 2109–2120.

Williams, E.L., Lim, S.H., Beers, S.A., Johnson, P.W., Strefford, J.C., Glennie, M.J., and Cragg, M.S. (2013a). Overcoming resistance to therapeutic antibodies by targeting Fc Receptors. Resistance to Immunotherapeutic Antibodies in Cancer. Strategies to Overcome Resistance Pubs Springer *2*, 49–71.

Williams, E.L., Tutt, A.L., Beers, S.A., French, R.R., Chan, C.H., Cox, K.L., Roghanian, A., Penfold, C.A., Butts, C.L., Boross, P., et al. (2013b). Immunotherapy targeting inhibitory Fcγ receptor IIB (CD32b) in the mouse is limited by monoclonal antibody consumption and receptor internalization. J. Immunol. *191*, 4130–4140.

Wong, A.L., and Lee, S.C. (2012). Mechanisms of Resistance to Trastuzumab and Novel Therapeutic Strategies in HER2-Positive Breast Cancer. Int. J. Breast Cancer *2012*, 415170.

Zhou, P., Comenzo, R.L., Olshen, A.B., Bonvini, E., Koenig, S., Maslak, P.G., Fleisher, M., Hoffman, J., Jhanwar, S., Young, J.W., et al. (2008). CD32B is highly expressed on clonal plasma cells from patients with systemic light-chain amyloidosis and provides a target for monoclonal antibody-based therapy. Blood *111*, 3403–3406.